

## Stereochemical Analysis by Solid-State NMR: Structural Predictions in Ambuic Acid

James K. Harper, Dewey H. Barich, Jian Z. Hu,<sup>†</sup> Gary A. Strobel,<sup>‡</sup> and David M. Grant\*

*Department of Chemistry, University of Utah, 315 South 1400 East, Salt Lake City, Utah 84112, Pacific Northwest National Laboratory, Richland, Washington 99352, and Department of Plant Sciences, Montana State University, Bozeman, Montana 59717*

*grant@chemistry.utah.edu*

*Received June 4, 2002*

Relative stereochemistry is predicted for ambuic acid using a novel solid-state NMR approach. This NMR technique entails a comparison of measured shift tensor principal values with computed values for all diastereomers, allowing the selection of a best-fit structure. The proposed method extends previous solution NMR structural data by simultaneously modeling with high statistical probability hydrogen-bonding arrangements and molecular conformation at two positions. A dimeric structure is proposed for ambuic acid based on the initial poor fit of the carboxyl carbon tensors to a monomeric model. The dimer model, consisting of hydrogen bonding between pairs of neighboring carboxyl groups, reduces the root mean square error at the carboxy tensor by a factor of 2.7. Lattice details are thus also described by the proposed approach. The structural characterization method presented is of general applicability and may be especially useful for characterizing difficult to crystallize or hydrogen-poor materials.

### Introduction

The determination of stereochemistry is an important part of the characterization of new materials, both of synthetic and natural origin. Typically, one of two methods is employed to address this problem. If single crystals of the material can be obtained, X-ray analysis provides relative stereochemistry and, if heavy atoms are present, absolute stereochemistry.<sup>1</sup> For materials not forming suitable crystals, solution NMR may allow determination of relative stereochemistry. NMR analysis, however, typically requires the presence of hydrogens and involves a measurement of the distances between different sites via a measurement of the nuclear Overhauser (NOE) interactions between proximate hydrogens.<sup>2</sup> Alternatively, NMR measurement of the three-bond proton-proton (i.e., H-C-C-H) scalar coupling constant (<sup>3</sup>J<sub>HH</sub>) allows the dihedral angle between hydrogens to be roughly estimated through the Karplus relationship.<sup>3</sup> For hydrogen-poor compounds or those forming microcryst-

alline powders, however, establishing stereochemistry remains a challenge.

Recently, we reported an alternative method for establishing relative stereochemistry using solid-state NMR methods.<sup>4</sup> This approach involves finding the best fit of measured shift tensor principal values with computed tensor values for all possible computer generated diastereomers using an *F* test. This technique potentially allows for the determination of relative stereochemistry even in microcrystalline or hydrogen-poor molecules. Initial application of this technique to the natural product terrein (**2**) correctly identified the relative stereochemistry with high statistical confidence.<sup>4</sup> It is interesting, however, that changes in both relative stereochemistry and conformation can strongly influence shift tensors. Thus, such conformational flexibility must also be included in a completely general approach. The essentially rigid structure of terrein precludes its use as a model for conformationally flexible molecules. Therefore, to more fully investigate the ability of shift tensors to predict stereochemistry when conformational diversity is present, we report application of our technique to ambuic acid (**1**).<sup>5</sup>

<sup>†</sup> Pacific Northwest National Laboratory.

<sup>‡</sup> Montana State University.

(1) Glusker, J. P.; Trueblood, K. N. *Crystal Structure Analysis*; Oxford: New York, 1985, Chapter 10.

(2) Neuhaus, D.; Williamson, M. P. *The Nuclear Overhauser Effect in Structural and Conformational Analysis*; VCH: New York, 1989.

(3) Karplus, M. A. *J. Am. Chem. Soc.* **1963**, *85*, 2870.

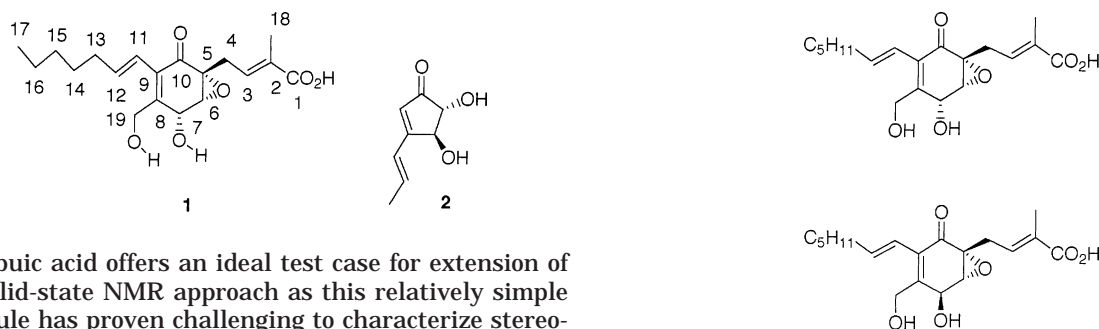
(4) Harper, J. K.; Mulgrew, A. E.; Li, J. Y.; Barich, D. H.; Strobel, G. A.; Grant, D. M. *J. Am. Chem. Soc.* **2001**, *123*, 9837.

(5) Li, J. Y.; Harper, J. K.; Grant, D. M.; Tombe, B. O.; Bashyal, B.; Hess, W. M.; Strobel, G. A. *Phytochemistry* **2001**, *56*, 463.

**TABLE 1. Chemical Shift Tensor Principal Values (ppm) for Ambuic Acid, Experiment (Theoretical<sup>a</sup>)**

carbon	solid-state $\delta_{iso}^b$	solution $\delta_{iso}^c$	$\delta_{11}$	$\delta_{22}$	$\delta_{33}$
1	171.0 (177.1)	171.2	247.1 (251.1)	157.3 (166.4)	108.4 (113.9)
2	132.4 (134.9)	131.9	231.6 (231.3)	120.9 (124.9)	44.8 (48.4)
3	134.1 (145.3)	136.6	245.0 (252.5)	131.5 (154.3)	25.7 (29.3)
4	24.9 (26.3)	28.8	31.2(35.3)	27.8 (29.8)	15.9 (13.8)
5	60.0 (60.1)	61.3	106.3 (107.1)	50.8 (57.0)	22.8 (16.3)
6	60.5 (59.7)	61.1	102.8 (98.3)	48.6 (52.8)	30.2 (28.0)
7	65.8 (68.6)	66.0	91.8 (91.5)	73.3 (74.2)	32.2 (40.0)
8	146.2 (161.2)	150.7	235.9 (242.5)	158.0 (185.9)	44.8 (55.1)
9	133.7 (133.4)	132.0	215.0 (205.8)	140.5 (147.9)	45.8 (46.7)
10	193.4 (199.8)	196.0	277.8 (281.2)	211.9 (221.4)	90.6 (96.7)
11	121.6 (128.7)	122.8	219.2 (223.9)	115.4 (120.0)	30.2 (42.3)
12	137.4 (147.7)	140.3	230.6 (244.7)	136.6 (158.7)	44.9 (39.5)
13 <sup>d</sup>	35.2 (38.8)	34.6	52.4 (57.2)	39.8 (40.9)	13.5 (18.4)
14 <sup>d</sup>	26.8 (33.9)	30.0	36.5 (52.5)	30.2 (38.8)	13.8 (10.4)
15 <sup>d</sup>	34.0 (34.9)	32.6	47.1 (53.6)	39.2 (40.8)	15.8 (10.2)
16	24.4 (25.7)	23.6	33.7 (37.7)	25.5 (29.0)	14.0 (10.4)
17	16.2 (15.6)	14.5	24.8 (26.2)	20.3 (22.0)	3.4 (-1.5)
18	14.2 (16.2)	13.0	25.8 (26.4)	10.2 (16.2)	6.6 (5.9)
19	62.0 (67.2)	60.3	86.6 (90.3)	71.1 (77.0)	28.3 (34.3)

<sup>a</sup>Theoretical shifts computed using a dimeric model, B3LYP/D95\* atomic positions and B3PW91/D95\*\* tensor values. Neutron diffraction data from related compounds were used to position carboxyl hydrogens and establish relative orientations of monomers as described in text. <sup>b</sup>Determined by averaging the FIREMAT principal values. <sup>c</sup>Established from an INADEQUATE analysis described elsewhere.<sup>5</sup> <sup>d</sup>Assignments shown are interchangeable.



Ambuic acid offers an ideal test case for extension of the solid-state NMR approach as this relatively simple molecule has proven challenging to characterize stereochemically. Extensive past attempts to obtain crystals of **1** suitable for X-ray analysis have failed. Further, the lack of suitable proton–proton interactions has prevented the solution NMR determination of relative stereochemistry as discussed elsewhere.<sup>5</sup> Tensor principal values for **1** were measured using the FIREMAT technique<sup>6</sup> (Table 1), providing the necessary experimental data to further investigate stereochemical determination by solid-state NMR.

## Results and Discussion

**<sup>13</sup>C Shift Assignments and Conformational Variety in Solid Ambuic Acid.** In ambuic acid, two diastereomers are possible as shown in Figure 1. However, before computed tensors for both structures may be compared with experiment, isotropic shifts must be correctly assigned to molecular positions. Shift assignments were made by first separating the lines into different carbon types (i.e., CH<sub>3</sub>, CH<sub>2</sub>, CH, or quaternary) based on a solid-state spectral editing analysis.<sup>7</sup> Within a given carbon type, isotropic lines that are widely separated ( $\geq 10$  ppm separation from a nearest neighbor) are assigned with the same relative ordering as found

**FIGURE 1.** Possible relative stereochemistries for ambuic acid.

in the solution (see solution shifts in Table 1). While differences in solution- and solid-state shifts for a given position are often observed, they are usually less than  $\pm 10$  ppm. For remaining shifts, all possible orderings of experiment with computed tensors are made within a subgroup of a given carbon type and the arrangement with the best fit retained. An *F* test assigns a confidence to any given assignment relative to other possibilities.<sup>4</sup> Using this method, most shifts in **1** were assigned at  $> 85\%$  probability. However, carbons 13, 14, and 15 could not be assigned at high confidence and the order shown is interchangeable.

Application of the proposed stereochemical determination method<sup>4</sup> to **1** must include the possibility of additional structures arising from conformational isomerism. Specifically, in addition to the two diastereomeric possibilities, the C8–C9–C11–C12 dihedral may be either  $0^\circ$  or  $180^\circ$  (the so-called *s-cis* or *s-trans* configurations, respectively), the C3–C4–C5–C6 dihedral angle also has considerable conformational flexibility, and the hydroxy hydrogens at C19 and C7 may assume a variety of conformations consistent with optimal hydrogen bonding. However, previous solution work<sup>5</sup> suggests that the C19 and C7 hydroxy groups form an intramolecular donor–acceptor arrangement to yield a highly favored<sup>8</sup> six-membered ring.

(6) Alderman, D. W.; McGeorge, G.; Hu, J. Z.; Pugmire, R. J.; Grant, D. M. *Mol. Phys.* **1998**, *95*, 1113.

(7) (a) Hu, J. Z.; Harper, J. K.; Taylor, C.; Pugmire, R. J.; Grant, D. M. *J. Magn. Reson.* **2000**, *142*, 326. (b) Wu, X.; Zilm, K. W. *J. Magn. Reson. A* **1993**, *102*, 205. (c) Wu, X.; Burns, S. T.; Zilm, K. M. *J. Magn. Reson. A* **1994**, *111*, 29.

In preparing model structures, at least two hydrogen-bonding conformations must be considered as a first approximation, one in which C19–OH acts as a donor with C7–OH as acceptor and the alternative in which C7–OH is the donor and C19–OH the acceptor. At C5, several conformational possibilities must also be considered due to rotation about the C4–C5 bond. However, the conformational possibilities about the C3–C4 bond are greatly restricted by the observation in solution of a  $^2J_{\text{HH}}$  coupling of 16 Hz at the C4 CH<sub>2</sub>.<sup>5</sup> According to the early work of Barfield and Grant,<sup>9</sup> a  $^2J_{\text{HH}}$  of this magnitude only allows a C2–C3–C4–C5 dihedral angle of 0° or 180°. Steric factors preclude the 0° structure due to an unfavorable approach of the region near C1 to the cyclohexenone ring and leave the 180° angle as the only feasible structure. Overall, an exhaustive consideration of all possible combinations of described conformations involves a prohibitive number of computations. Fortunately, in most cases, the chemical shift is a reflection primarily of local structure,<sup>10</sup> suggesting that some parts of the molecule may be adjusted without influencing the tensors in more distant fragments (typically more than three bonds removed). Using this assumption, eight model structures were prepared in which all combinations of relative stereochemistry, hydrogen bonding and conformation about the C9–C11 bond were investigated (see Figure 2). This approach allows the initial conformation about the C4–C5 bond to be determined by an energy minimization procedure. An additional fine adjustment about C4–C5 is subsequently made using shift tensor data once other structural details are established.

**High Probability Structural Assignments in Ambuic Acid.** Ideally, structural variations to be examined would be separated by several bonds from one another, allowing unique molecular moieties to be examined independently. In practice, this can be approximated by analyzing only tensor values from carbons directly attached to chiral centers or to bonds forming rotation axes for conformational changes. Tensors from such carbons most strongly reflect structural changes, as electronic differences are typically greatest in the vicinity of the variation. This approach thus approximates an isolated structural feature. Inclusion of more distant carbons usually has a significantly smaller effect and such carbons are omitted from analysis here.<sup>4</sup> For establishment of hydrogen-bonding arrangement, only tensors for C19 and C7 are therefore compared with theory. Likewise only C5, C6, and C7 principal values are used to establish stereochemistry and C4 and C5 for predicting conformation about the C4–C5 bond. In the case of rotation about the C9–C11 bond, however, it is necessary to include C8, C9, C11, and C12 as  $\pi$ -delocalization of electrons makes it difficult to isolate C8 and C12 from the electronic effects of the conformational changes.

A comparison of computed tensors for C8, C9, C11, and C12 with experimental data for the eight model structures shows that the *s-cis* geometry is preferred at roughly the 85% probability level over the next best *s-trans* model. This probability level corresponds to a fit

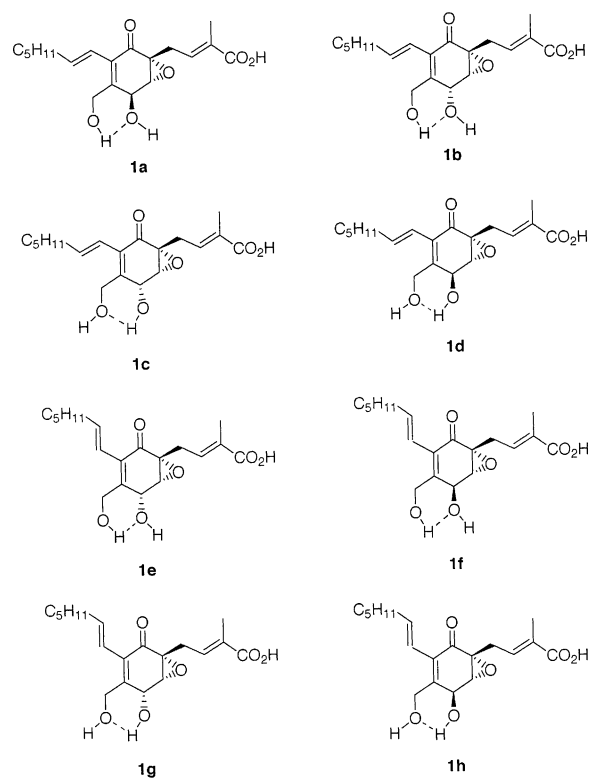


**FIGURE 2.** Eight model structures of ambuic acid prepared for comparison with experimental data. In each case, the model structure was constructed and partially optimized via an energy minimization procedure and the corresponding tensor computed for comparison.

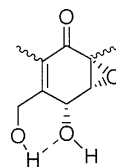


**FIGURE 3.** Proposed hydrogen-bonding arrangement at C7 and C19 in ambuic acid. This bonding order independently supports previous solution predictions and is preferred over an arrangement having C7–OH as donor with the C19–OH as the acceptor at the 90% probability level.

of the *s-cis* computed tensors to experimental data that is 1.44 standard deviations ( $\sigma$ ) better than the corresponding *s-trans* model. The number of potentially correct structures is thus reduced to four (structures **1a–d**) by the selection of the *s-cis* arrangement (or, more correctly, a skew arrangement as described below). Comparing computed tensors at C5, C6, and C7 with experiment for the four remaining structures allows the stereochemistry to be determined. The  $5R^*,6R^*,7R^*$  stereochemistry was found to fit the experimental data best and is preferred over **1a** or **1d** ( $5S^*,6S^*,7R^*$ ) at roughly the 82% confidence level (i.e., a better fit by  $1.34\sigma$ ). The remaining structures **1b** and **1c** involve selection of a hydrogen-bonding arrangement at C7 and C19. Structure **1b**, having C19–OH as hydrogen bond donor with C7–OH as acceptor, was found to be best at approximately the 90% confidence level (Figure 3) corresponding to a  $1.65\sigma$  better fit. The high quality fits of measured tensors at C19 and C7 with models describing

(8) Etter, M. C. *Acc. Chem. Res.* **1990**, *23*, 120.

(9) Barfield, M.; Grant, D. M. *J. Am. Chem. Soc.* **1963**, *85*, 1899.

(10) Pretsch, E.; Clerc, T.; Seibl, J.; Simon, W. *Tables of Spectral Data for Structural Determination of Organic Compounds*; Springer-Verlag: New York, 1989; pp c10–c265.

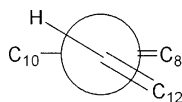


**FIGURE 4.** Skew conformation predicted for the C8–C9–C11–C12 dihedral angle.

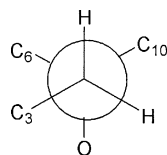


**FIGURE 5.** Newman projection of the best-fit C3–C4–C5–C6 dihedral angle.

intramolecular hydrogen bonding independently supports the previous solution prediction of such hydrogen bonding.<sup>5</sup>

The observation of a near *s-cis* geometry in **1** is unexpected as 1,3-butadiene is found to consist primarily of the *s-trans* structure.<sup>11</sup> In 1,3-butadiene, the *s-trans* conformation is preferred over the *s-cis* or near *s-cis* arrangements by an estimated 2–5 kcal/mol.<sup>12</sup> This preference is usually ascribed to unfavorable van der Waals interactions in the *s-cis* arrangement not found in *s-trans*. However, in **1** the best-fit C8–C9–C11–C12 dihedral angle is found to be a nearly *s-cis* geometry corresponding to the skew conformation shown in Figure 4. This preference for the *s-cis* arrangement appears to arise from unfavorable steric interactions in the *s-trans* geometry of the hydrogen at C12 with the carbonyl oxygen at C10. Less serious proton–proton interactions are also found for the strictly planar *s-cis* geometry due to the protons on C12 interacting with those on C19. The skew conformation relaxes these unfavorable interactions and is thus preferred.

With the stereochemistry, hydrogen bonding and C8–C9–C11–C12 dihedral angle established, the C3–C4–C5–C6 dihedral angle may be determined to complete the characterization. A comparison of 12 model structures differing in the C3–C4–C5–C6 dihedral angle gave a best fit to experimental data at  $60^\circ \pm 44^\circ$  (Figure 5). All structures considered retained the previously established features of **1b**. These models define a  $0^\circ$  starting point in which the C3–C4 bond is eclipsed with the C5–C6 bond. Subsequent rotations about the C4–C5 bond were made in  $30^\circ$  increments and define a positive rotation as initially moving the C3 toward the epoxide oxygen. All model structures were constructed and energy minimized with the C3–C4–C5–C6 dihedral angle fixed and tensors computed. The relatively large error in the C3–C4–C5–C6 angle may reflect the neglect of hydrogen bonding at the carboxyl group as discussed in the following section.

The proposed methodology is thus capable of establishing both relative stereochemistry and associated conformational variation. The final structure chosen is the statistically most probable structure rather than an

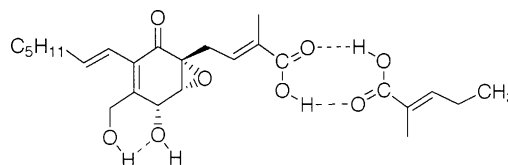


**FIGURE 6.** Best-fit dimeric structure proposed for ambuic acid. This model shows all predicted structural features including hydrogen-bonding arrangements, stereochemistry, and molecular conformations at two positions. The neighboring fragment was constructed using structural parameters from the complete molecule and the  $\alpha$ ,  $\beta$ ,  $\gamma$ , and  $\delta$  substituents to the carboxyl group.

unambiguous experimentally determined structure. As applied here, the method involves a stepwise elimination of potential structures. The path chosen selects as the first step the geometry variation causing the greatest change in principle values. Subsequent steps are taken using the second largest variation, and continue in this manner until all features are addressed. Had the proposed approach using only carbons directly attached to varying groups resulted in truly isolated fragments, any path would result in the same structure. For **1**, however, the structure chosen requires that the largest shift variations be considered first. This dependence on sequence demonstrates that the fragments examined are not truly isolated and suggests that future alternative approaches to structure may yet improve analysis as discussed below.

**Evidence for a Dimeric Hydrogen-Bonding Structure.** While the proposed structure of **1** is strongly preferred over other potentially correct structures, not all computed carbons tensors in the final structure fit experimental values. The fit to the carboxyl carbon at C1 is especially poor. The deficiencies at C1 may arise either from modeling the ionization state incorrectly (i.e., the free acid rather than the salt) or from the neglect of hydrogen bonding. Ambuic acid was demonstrated to be the free acid by elemental analysis, eliminating the possibility of errors in the ionization state. A dimeric computer model was therefore prepared in which a fragment of **1** was placed in hydrogen bonding position (as determined from neutron diffraction data of related structures)<sup>13</sup> with the carboxyl group of a neighboring ambuic acid molecule (Figure 6). Tensors computed for this dimer fit experiment significantly better than the free acid alone with a root mean square (rms) error of 7.5 ppm for C1 of the dimer vs 20.4 ppm for the monomer (Figure 7). Hence, in carboxylic acids where strong hydrogen bonding occurs, it appears to be necessary to include the hydrogen-bonded partner to accurately model the shift tensors. Overall, the rms error in computed tensors for the final proposed dimer of **1** is 8.3 ppm. Approximately one-third of this error arises from poor modeling of six tensor values at certain  $sp^2$  carbons. This inability to compute accurate tensors for all  $sp^2$  carbons has been previously observed<sup>4,14</sup> and identifies a current shortcoming of the computational methods. A dimer of **1** displaying all predicted structural features is shown in Figure 6.

(11) (a) Almenningen, A.; Bastian, O.; Traetteburg, M. *Acta Chem. Scand.* **1958**, *12*, 1221. (b) Kuchitsu, K. K.; Fukuyama, T.; Morino, Y. *J. Mol. Struct.* **1967**, *1*, 643. (c) Lipnick, R. L.; Garbisch, E. W. *J. Am. Chem. Soc.* **1973**, *95*, 6370.

(12) Devaquet, A. J. P.; Townshend, R. E.; Hehre, W. J. *J. Am. Chem. Soc.* **1976**, *98*, 4068.

(13) Leiserowitz, L. *Acta Crystallogr.* **1976**, *B32*, 775.

(14) Harper, J. K.; Grant, D. M. *J. Am. Chem. Soc.* **2000**, *122*, 3708.

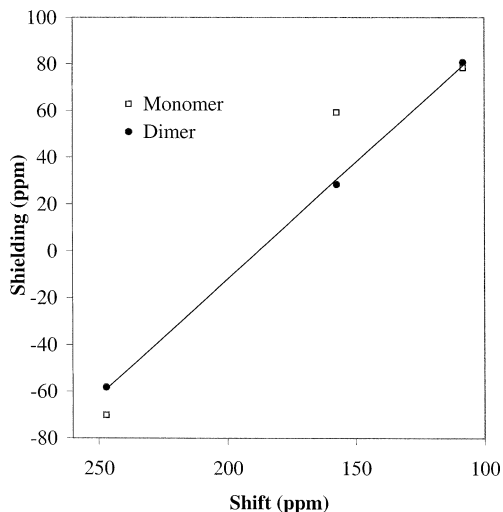


**FIGURE 7.** Correlation plot illustrating the fit of both a dimeric and a monomeric model to experimental C1 principal values. The dimeric model provides a better fit to experimental data by a factor of 2.7 and is thus strongly preferred.

The NMR prediction of a dimeric solid-state structure for ambuic acid may also offer insight into the reluctance of ambuic acid to crystallize. The dimeric structure requires that carboxyl groups pair, leaving long hydrocarbon tails to interact in other regions of the lattice. The potentially orienting influence of hydrogen bonds is also removed by the formation of an intramolecular hydrogen bond at C19 and C7. Work on polyethylene and other long-chain polymers have found that such systems lack strong orienting influences and often have disorder.<sup>15</sup> Nevertheless, the narrow lines of the solid-state isotropic spectrum indicate that **1** forms a well-defined lattice but lacks the long-range order necessary for the formation of larger crystals.

**Alternative Analysis Schemes.** The scheme used here of including only certain carbons to establish a given structural feature represents a conservative approach. This path was chosen because of the close proximity of other groups and uncertainty about the interplay between conformation, stereochemistry and hydrogen bonding. Future analyses may potentially be enhanced by changes in three areas. The first involves the inclusion of all combinations of conformational changes. This was presently avoided due to the great increase in number of computations needed. For example, ninety-six times more structures must be considered if all conformational models about the C4–C5 bond are included for each of the structures **1a–h**. Second, statistical analysis may be extended to include all carbons that reflect a given conformational change. Theoretical studies of conformation versus shift presently suggest that conformational changes are reflected primarily in the  $\alpha$  and  $\beta$  positions with the  $\alpha$  position showing the largest effect.<sup>14,16</sup> Variations at  $\gamma$  positions are usually comparable to the errors in the computed shifts and must thus be excluded. Therefore comparisons that includes all  $\alpha$  and  $\beta$  carbons

may allow for more accurate structural predictions. In contrast, analyses that include all carbons in a molecule are likely to be less informative due to dilution by those segments of a structure that are insensitive to the change. Finally, alternative statistical figures of merit may also be considered. However, the  $F$  test, used here, has the advantage of being relative tolerant of systematic errors since such errors will be present in both structures being compared and will thus cancel in the ratio used to obtain an  $F$  value. The  $z$ -surface approach of Oldfield also displays this tolerance of systematic errors for a similar reason.<sup>17</sup>

## Conclusions

Application of the proposed solid-state NMR and computational methods allows a high probability structural assignment of **1**. In this case, local structural details are obtained for four previously uncharacterized features involving stereochemistry, hydrogen bonding, and molecular conformation. A full verification of all predictions must await future X-ray analysis. However, a recent synthesis of both diastereomers of ambuic acid has confirmed the prediction of relative stereochemistry made here.<sup>18</sup> Statistically, the prediction of stereochemistry ranks as one of the least confidently known of the assignments made. The independent synthetic support for the proposed stereochemistry is thus encouraging and lends credibility to the other more statistically probable structural features. The techniques described here may also be used with isotropic shifts rather than principal shift values. However, isotropic values typically exhibit smaller differences for a given structural change than principal values and are thus generally less statistically reliable for structural predictions as discussed previously.<sup>4</sup>

## Experimental Section

Ambuic acid was obtained from the endophytic fungus *Pestilotiopsis microspora* as previously described.<sup>5</sup>

FIREMAT <sup>13</sup>C data for **1** were collected on a CMX-400 Chemagnetics spectrometer operating at 100.62 MHz. The spectrum was acquired with TPPM <sup>1</sup>H decoupling<sup>19</sup> at a frequency of 400.12 MHz, a 180° pulse of 8.2  $\mu$ s and a 20° phase angle separating adjacent pulses. Spectral widths of 18.5 and 110.9 kHz were collected for the evolution and acquisition dimensions, respectively. A <sup>1</sup>H 90° pulse width of 4.1  $\mu$ s was used together with a <sup>13</sup>C 180° pulse of 7.8  $\mu$ s. A total of 32 evolution increments of 1152 scans each were collected with a 3 s recycle time for a total experiment time of 1.3 days. Evolution dimension data was extended to 9216 points using the previously described replication scheme inherent in the FIREMAT approach.<sup>6</sup> Digital resolutions of 12.03 Hz per point were obtained in both dimensions after the replication. A spinning speed of 578 Hz was used, and the spectrum was externally referenced to the high frequency peak of adamantane at 38.56 ppm. Tensor values in all FIREMAT analyses were obtained using previously described procedures and software.<sup>6,20</sup>

(17) Le, H.; Pearson, J. G.; de Dios, A. C.; Oldfield, E. *J. Am. Chem. Soc.* **1995**, *117*, 3800.

(18) Li, C.; Porco, J. A., Jr. Unpublished results, Boston University.

(19) Bennett, A. E.; Reinstra, C. M.; Auger, M.; Lakshmi, K. V.; Griffin, R. J. *J. Chem. Phys.* **1995**, *103*, 6951.

(20) Sethi, N. K.; Alderman, D. W.; Grant, D. M. *Mol. Phys.* **1990**, *71*, 217.

(15) (a) Schmidt-Rohr, K.; Spiess, H. W. *Multidimensional Solid-State NMR and Polymers*; Academic Press: San Diego, 1994; Chapter 5.

(16) Facelli, J. C.; Orendt, A. M.; Jiang, Y. J.; Pugmire, R. J.; Grant, D. M. *J. Phys. Chem.* **1996**, *100*, 8268.

Tensor calculations were on structures that had been partially optimized via the B3LYP<sup>21</sup> method employing the D95\* basis set. Gauge invariant<sup>22</sup> tensor computations were preformed at the B3PW91<sup>21a,23</sup>/D95\*\* level of theory using parallel processing and the Gaussian 98 program.<sup>24</sup> Computed shieldings were converted to shifts using the previously established relationships<sup>25</sup>  $\text{shift} = (\text{shielding} - 194.933)/-$

(21) (a) Becke, A. D. *J. Chem. Phys.* **1993**, *98*, 5648. (b) Lee, C.; Yang, W.; Parr, R. G. *Phys. Rev. B* **1988**, *37*, 785.

(22) Ditchfield, R. *Mol. Phys.* **1974**, *27*, 789.

(23) Perdew, J. P.; Wang, Y. *Phys. Rev. B* **1992**, *45*, 13244.

(24) Frisch, M. J.; Trucks, G. W.; Schlegel, H. B.; Scuseria, G. E.; Robb, M. A.; Cheeseman, J. R.; Zakrzewski, V. G.; Montgomery, J. A., Jr.; Stratmann, R. E.; Burant, J. C.; Dapprich, S.; Millam, J. M.; Daniels, A. D.; Kudin, K. N.; Strain, M. C.; Farkas, O.; Tomasi, J.; Barone, V.; Cossi, M.; Cammi, R.; Mennucci, B.; Pomelli, C.; Adamo, C.; Clifford, S.; Ochterski, J.; Peterson, G. A.; Ayala, P. Y.; Cui, Q.; Morokuma, K.; Malick, D. K.; Rabuck, A. D.; Raghavachari, K.; Foresman, J. B.; Cioslowski, J.; Ortiz, J. V.; Baboul, A. G.; Stefanov, B. B.; Liu, G.; Liashenko, A.; Piskorz, P.; Komaromi, I.; Gomperts, R.; Martin, R. L.; Fox, D. J.; Keith, T.; Al-Laham, M. A.; Peng, C. Y.; Nanayakkara, A.; Challacombe, M.; Gill, P. M. W.; Johnson, B.; Chen, W.; Wong, M. W.; Andres, J. L.; Gonzales, C.; Head-Gordon, M.; Replogle, E. S.; Pople, J. A. *Gaussian 98*, Revision A.9; Gaussian, Inc.: Pittsburgh, PA, 1998.

(25) Harper, J. K. In *Encyclopedia of NMR*; Grant, D. M., Harris, R. K., Eds.; Wiley: Chichester, 2002; Vol. 9, pp 589–597.

1.006 for sp<sup>2</sup> carbons and  $\text{shift} = (\text{shielding} - 190.325)/-1.031$  for sp<sup>3</sup> carbons.

An elemental analysis was performed on **1** to establish sodium content. The analysis was performed by CALI labs in duplicate on 7.26 and 11.64 mg samples and showed less than 0.15% sodium present in both cases, consistent with the predicted free acid form of **1**.

**Acknowledgment.** Support for this research was provided by the National Institutes of Health under Grant No. GM 08521-40 to D.M.G. and an NSF grant to G.A.S. Computer support for all tensor computations was provided by the Center for High Performance Computing at the University of Utah. Photo of the plant courtesy of Gary Strobel, Montana State University, and the SEM of *P. microspora* was provided by W. M. Hess, Brigham Young University.

**Supporting Information Available:** Computed structures (Cartesian coordinates) and corresponding shielding tensors for the 20 structures and one dimer considered. This material is available free of charge via the Internet at <http://pubs.acs.org>.

JO020377I